ELSEVIER

Journal of Non-Crystalline Solids 274 (2000) 62–68

JOURNAL OF NON-CRYSTALLINE SOLIDS

www.elsevier.com/locate/jnoncrysol

Controlling the optical constants of thermally-evaporated $Ge_{10}Sb_{30}S_{60}$ chalcogenide glass films by photodoping with silver

E. Márquez [a,*], T. Wagner [b], J.M. González-Leal [a], A.M. Bernal-Oliva [a], R. Prieto-Alcón [a], R. Jiménez-Garay [a], P.J.S. Ewen [c]

[a] *Departamento de Física de la Materia Condensada, Facultad de Ciencias, Universidad de Cádiz, P.O. Box 40, 11510 Puerto Real (Cádiz), Spain*

[b] *Department of General and Inorganic Chemistry, Faculty of Chemical Technology, University of Pardubice, 53210 Pardubice, Czech Republic*

[c] *Department of Electrical Engineering, University of Edinburgh, EH9 3JL Edinburgh, UK*

Abstract

We have analysed the effect of silver content on the optical properties of Ag-doped $Ge_{10}Sb_{30}S_{60}$ chalcogenide glass films; the chalcogenide host layers were prepared by vacuum thermal evaporation. Films of compositions $Ag_x(Ge_{0.1}Sb_{0.3}S_{0.6})_{100-x}$, with $x \lesssim 8$ at.%, were obtained by successively photodissolving thin (around 10 nm) layers of silver. The optical constants (n,k) have been determined by a method based on the envelope curves of the optical transmission spectrum at normal incidence. The dispersion of the refractive index of the Ag-photodoped chalcogenide films is analysed within the single-effective-oscillator approach. The optical-absorption data indicate that the absorption mechanism is non-direct transition. We found that the refractive index of the Ag-doped samples increases with the Ag content, whereas the optical band gap, E_g^{opt}, decreases from 1.97 ± 0.01 to 1.67 ± 0.01 eV. These results are consistent with the hypothesis that the photodoped Ag is a structure modifier in the *a*-$Ge_{10}Sb_{30}S_{60}$ films.

1. Introduction

The photoinduced solid-state chemical reaction between various metals (e.g., Ag, Cu or Zn) and chalcogenide glasses (also known as photodoping, photodissolution or photodiffusion) has been widely studied [1–5]. However, at present, the mechanism for this phenomenon is still speculative to our knowledge. Silver-doped chalcogenide glasses have been investigated mainly for their potential applications as optical recording materials and, more recently, as materials for diffractive optics and optical integrated circuits for IR operation [6]. All these applications require the fabrication of structures in a range of thicknesses, from one to tenths of a micron. Understanding the kinetics of the photodissolution process and finding new suitable host glass-matrices are crucial points for these technological applications. In the present

* Corresponding author. Tel.: +34-95 601 6318; fax: +34-95 601 6288.

E-mail address: emilio.marquez@uca.es (E. Márquez).

0022-3093/00/$ - see front matter
PII: S0022-3093(00)00184-8

study we have analysed the effect of photodoping with Ag, on the optical properties of $Ge_{10}Sb_{30}S_{60}$ ternary chalcogenide glass films.

2. Experimental

The chalcogenide host layers were deposited using the vacuum thermal evaporation technique. To produce the glass for the evaporation source, the constituents were measured into a quartz tube, vacuum-sealed and melted in a rocking furnace for 24 h at 1000°C and subsequently quenched in air. Fragments of the material were used to prepare the layers in a chamber with a pressure of 1×10^{-4} Pa, at a rate of 1 nm s^{-1} (the deposition rate was measured by the dynamical weighing procedure). The thickness of the films ranged between 1000 and 1500 nm, which are appropriate for the evaluation of the optical parameters by the present characterization method. Subsequently, different layers of silver were deposited on top of the chalcogenide host. For the silver evaporation we used an Al_2O_3-covered tungsten boat, thereby reducing the heat and light exposure of the samples during deposition. Photodoping was carried out by illuminating the samples in a mask aligner (Karl Suss MJB3 UV400), equipped with a 200 W Hg lamp. During light exposure the samples were sandwiched between two other glass plates to reduce surface oxidation.

The silver concentration of our samples was $\lesssim 8$ at.%. When preparing layers with a large silver content, we found that photodissolving a thick layer of Ag in one step resulted in a photodoped product that was inhomogeneous. However, doping the host step-by-step, by consecutively dissolving $\sim$10 nm layers, produced a homogeneous film. The silver concentrations were determined from measurements of the silver and chalcogenide layer thicknesses.

The optical transmission and reflection spectra (at normal incidence) of the films were recorded with a ultraviolet/visible/near infrared spectrophotometer (Perkin Elmer, model λ-9). It should be noted that the transmission spectra of the doped thin-film samples were those corresponding to homogeneous isotropic weakly-absorbing layers, with uniform thickness; it is also important to mention that in the transparent region, the sum of transmission and reflection spectra was 100%, within experimental error, for all photodoped samples. These results confirmed the homogeneity of the doped samples and the absence of silver remaining on top of the chalcogenide host, after illumination. The thickness of the films was measured by a mechanical stylus (Sloan, model Dektak IIA), with an accuracy of ±5 nm, for the purpose of comparison with the results deduced from the transmission spectra.

3. Determination of the optical constants

To calculate the refractive index, n, and extinction coefficient, k, we used a method suggested by Swanepoel [7]. The optical constants are obtained by using only the transmission spectrum. The layer is assumed to be homogeneous and with uniform thickness. Otherwise, there should be a shrinking in the interference fringes of the optical transmission spectrum [8,9]. In the present case such shrinkage is not observed.

According to Swanepoel's method, which is based on the approach of Manifacier et al. [10] of creating the upper and lower envelopes of the transmission spectrum, the refractive index in the region where the absorption coefficient, α, is ≈0, was calculated by the expression [7]

$$n = \sqrt{N + \sqrt{N^2 - s^2}}, \tag{1}$$

where

$$N = 2s\frac{T_{\max} - T_{\min}}{T_{\max}T_{\min}} + \frac{s^2+1}{2}$$

with s the refractive index of the substrate. $T_{\max}$ and $T_{\min}$ are, respectively, the envelope values at the wavelengths in which the upper and lower envelopes and the experimental transmission spectrum are tangent, as shown in Fig. 1. The first ns are calculated using Eq. (1) at the wavelengths corresponding to the tangent points. The accuracy to which λ can be measured is ±1 nm. The maximum absolute accuracy of $T_{\max}$ and $T_{\min}$ is ±0.001.

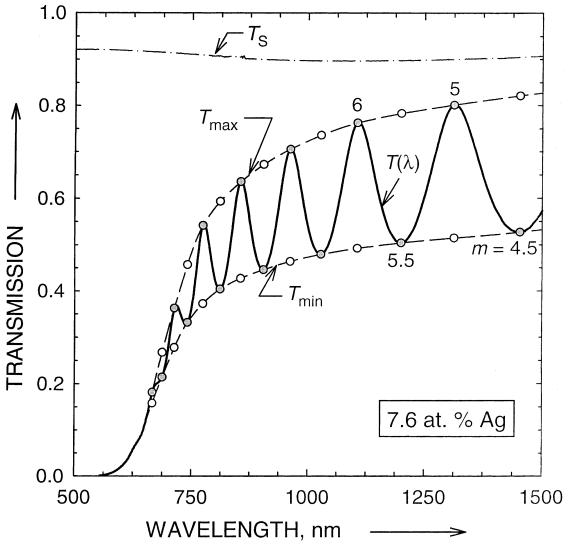

Fig. 1. Optical transmission spectrum, $T(\lambda)$, for a Ag-photodoped $Ge_{10}Sb_{30}S_{60}$ chalcogenide glass thin film with a silver content of 7.6 at.%. The top, T_{max}, and bottom, T_{min}, envelope curves have been computer drawn using the useful algorithm developed by McClain et al. [11]. T_s is the transmission spectrum of the bare substrate. The order numbers for some tangent points are conveniently marked.

If n_1 and n_2 are the refractive indices at two adjacent tangent points at wavelengths λ_1 and λ_2, using the basic equation for interference fringes:

$$2nt = m\lambda, \tag{2}$$

where m is an order number, the thickness is given by

$$t = \frac{\lambda_1\lambda_2}{4(\lambda_1 n_2 - \lambda_2 n_1)}. \tag{3}$$

It should be noted that, owing to the optical absorption, Eqs. (2) and (3) are not valid at the interference maxima and minima, but are valid at the tangent points referred to previously [8]. A set of ts is obtained solving Eq. (3) for each pair of consecutive tangent points. The mean t so calculated is used together with the first refractive indices, to determine the order numbers from Eq. (2): m being an integer for an upper tangent point and a half-integer for a lower tangent point. More accurate ts (t_{acc}s) are obtained by taking the corresponding integral and half-integral ms. Using these ms and the mean t_{acc}, a set of ns (n_{acc}s) are again calculated.

The absorption coefficient can be determined from the relation [7]

$$x = \exp(-\alpha t),$$

where x is the absorbance, given by

$$x = \frac{E_M - \sqrt{E_M^2 - (n^2-1)^3(n^2-s^4)}}{(n-1)^3(n-s^2)} \tag{4}$$

and

$$E_M = \frac{8n^2 s}{T_{max}} + (n^2-1)(n^2-s^2).$$

Finally, the extinction coefficient can be determined from the relation: $k = \alpha\lambda/4\pi$ [7].

4. Results

The t_{acc}s and n_{acc}s for a representative photodoped $Ge_{10}Sb_{30}S_{60}$ sample, in which the silver content was 7.6 at.%, are shown in Table 1. The maximum possible error in n varies from ± 0.004 to ± 0.011. We emphasize that the thickness of the films measured by the profilometer, is close to that calculated from the transmission spectra. For instance, for the film with metal content 7.6 at.%, the measured thickness is 1223 ± 24 nm, whereas 1242 ± 7 nm is calculated.

The data on the dispersion of the refractive index, $n(\lambda)$, were evaluated according to the single-effective-oscillator model proposed by Wemple and DiDomenico [12,13]. These authors investigated dispersion data for more than a hundred different materials, both covalent and ionic, crystalline and amorphous. They found that all the data could be described, to an excellent approximation, by the following formula:

$$n^2(\hbar\omega) = 1 + \frac{E_d E_o}{E_o^2 - (\hbar\omega)^2}, \tag{5}$$

where $\hbar\omega$ is the photon energy, E_o is the oscillator energy and E_d is the oscillator strength or dispersion energy. Plotting $(n^2-1)^{-1}$ against $(\hbar\omega)^2$ allows us to determine the oscillator parameters, by

Table 1
Values of λ, T_{max}, T_{min}, t_{acc} and n_{acc} for the transmission spectrum of Fig. 1

λ (nm) (±1 nm)	T_{max} (±0.001)	T_{min} (±0.001)	t_{acc} (nm)	n_{acc}
1624	0.841	0.549	1260	2.615 (±0.004)
1453	0.822	0.527	1242	2.632 (±0.005)
1313	0.801	0.515	1237	2.643 (±0.005)
1200	0.783	0.505	1239	2.657 (±0.005)
1106	0.763	0.493	1237	2.671 (±0.005)
1028	0.736	0.479	1239	2.690 (±0.005)
962	0.706	0.464	1241	2.711 (±0.006)
904	0.672	0.446	1241	2.729 (±0.006)
855	0.636	0.428	1244	2.754 (±0.007)
811	0.594	0.404	1240	2.775 (±0.008)
774	0.542	0373	1229	2.804 (±0.009)
741	0.457	0.332	1249	2.834 (±0.011)

$\bar{t}_{acc} = 1242$ nm, $\sigma_{n-1} = 7$ nm (0.6%)

fitting a linear function to the smaller energy data. All these plots are shown in Fig. 2. As was pointed out by Wemple and DiDomenico [12], deviations from the linear relationship result from the proximity of the band edge (interband absorption), at larger photon energies. The dependence of the single-effective-oscillator parameters on silver content is shown in Fig. 3; the Ag content dependence of the static refractive index, $n(\hbar\omega = 0)$, is also displayed in Fig. 3.

The optical gap, E_g^{opt}, was determined from the intercept on the energy axis of the linear fit of the larger energy data, in a plot of $(\alpha\hbar\omega)^{1/2}$ versus $\hbar\omega$ (Tauc extrapolation [14]) – all the corresponding Tauc plots are shown in Fig. 4. In Fig. 5 we show the dependence of the Tauc gap on Ag content. The decrease of E_g^{opt}, from 1.97 ± 0.01 to 1.67 ± 0.01 eV, is explained by the fact that the binding energy of the Ag–S bonds, 217.1 kJ mol^{-1}, is much smaller than that of the Ge–S and Sb–S

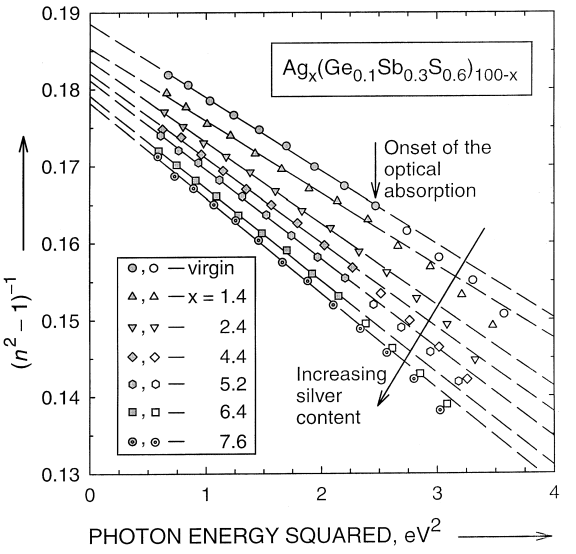

Fig. 2. Wemple–DiDomenico fits of the optical-dipersion data. The solid lines are linear fits.

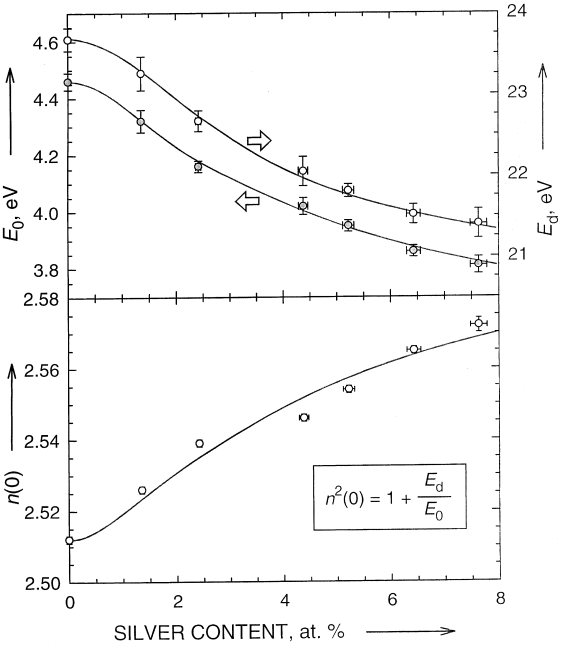

Fig. 3. Silver-content dependence of the single-effective-oscillator parameters E_o and E_d. Also, the variation of the static refractive index, $n(\hbar\omega = 0)$, with Ag content. All the solid lines are to guide the eye.

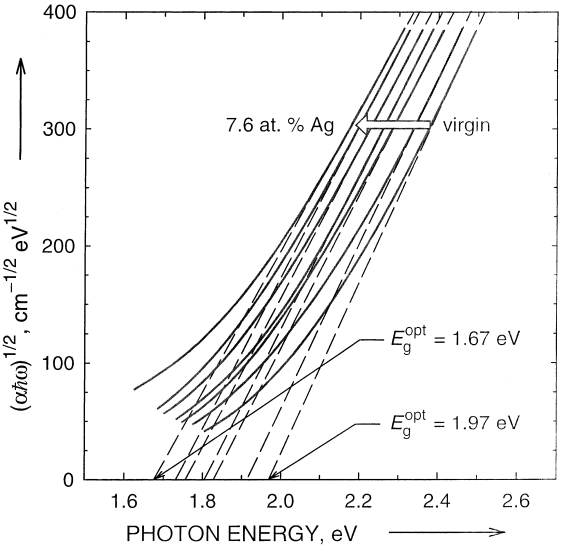

Fig. 4. Determination of the optical band gap, E_g^{opt}, in terms of the Tauc law.

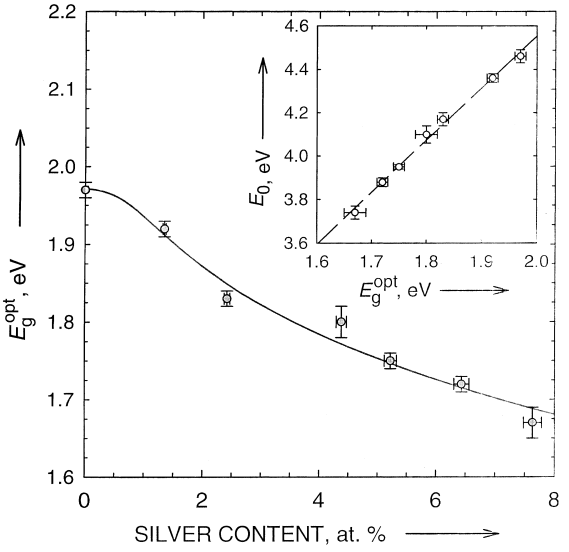

Fig. 5. Tauc gap versus silver content in the $Ag_x(Ge_{0.1}Sb_{0.3}S_{0.6})_{100-x}$ glassy system. The solid line is to guide the eye. In the inset, E_o versus E_g^{opt} (scaling between the two optical parameters). In this case, the dashed line is a linear fit (the value of the slope is 2.40).

bonds, 551.0 and 378.7 kJ mol^{-1}, respectively [15]. Therefore, there is a smaller energy splitting between the states of the valence and conduction bands.

5. Discussion

The oscillator energy, E_o, is an 'average' energy gap (Wemple–DiDomenico 'gap') [12,13] and to a good approximation it varies in proportion to the Tauc gap, as was found by Tanaka when investigating the As_xS_{100-x} glassy system [16] and more recently by Kosa et al. [17] in the case of Ag-doped $As_{33}S_{67}$ glass films. From the inset of Fig. 5, the relationship $E_o \approx 2.40 \times E_g^{opt}$, is deduced. On the other hand, the dispersion energy, E_d, serves as a measure of the strength of interband transitions. An important achievement of the Wemple–Di-Domenico model is that it relates the dispersion energy to other physical parameters of the material through an empirical formula [12,13]:

$$E_d = \beta N_c Z_a N_e \ (\mathrm{eV}), \tag{6}$$

where β is a two-valued constant with either an 'ionic' or a 'covalent' value ($\beta_i = 0.26 \pm 0.03$ eV and $\beta_c = 0.37 \pm 0.04$ eV, respectively), N_c the coordination of the cation nearest neighbor to the anion, Z_a the formal chemical valency of the anion and N_e is the total number of valence electrons (cores excluded) per anion.

Fig. 3 shows that E_d decreases with increasing Ag content. Eq. (6) was successfully applied by Tanaka [16], to explain the increase of E_d with increasing As content in the As_xS_{100-x} binary glassy system (owing to the increase in the effective coordination of the cation). More recently, Kosa et al. [17] extended the validity of Eq. (6), to explain the increase of the dispersion energy of the Ag-doped a-$As_{33}S_{67}$ films, with increasing Ag content. In this particular case, it was assumed that the overall (average) cation coordination is the factor, which is most affected by the addition of silver to the amorphous structure. This idea was supported by the fact that the composition of the samples at larger silver concentration, is definitely close to those of the ternary crystalline compounds such as trechmannite, $AgAsS_2$ (25 at.% of Ag) and proustite, Ag_3AsS_3 (42 at.% of Ag).

From Eq. (6), a cation coordination number, N_c, can be estimated for the virgin sample using the relationship: $N_c = E_d/\beta Z_a N_e$, where in this

particular case, $Z_a = 2$ and $N_e = (4 \times 10 + 5 \times 30 + 6 \times 60)/60 = 55/6$. Thus, $N_c \approx 3.23$. This N_c is in agreement with that which would be expected for the $Ge_{10}Sb_{30}S_{60}$ chalcogenide glass. In fact, if we rewrite this chemical composition in the form $(Ge_{0.25}Sb_{0.75})_{40}S_{60}$, a hypothetical 'cation' such as $Ge_{0.25}Sb_{0.75}$ could now be considered. For this 'cation', N_c could be obtained as follows: $N_c^{theo} = 4 \times 0.25 + 3 \times 0.75 = 3.25$. For a general glassy composition $Ge_xSb_yS_z$, if only heteropolar chemical bonds are considered, the expression $4x + 3y = 2z$ should be verifiable. Then, taking $N_c^{theo} = 3.25$, that we have previously derived, this last equation leads to a composition such as $Ge_9Sb_{29}S_{62}$. It is known [18] that $Ge_xSb_{0.4-x}S_{0.6}$ thin films contain some homopolar M–M bonds, whose population increases with increasing 'x'. Thus, Ge-rich ternary films such as $Ge_{30}Sb_{10}S_{60}$ contain a larger quantity of those bonds than the films that have been used in this work. This particular fact is consistent with the agreement we have found between the N_c calculated from Wemple's equation and that derived theoretically, N_c^{theo}, in the form described above.

The incorporation of Ag into the structure of the present Ge–Sb–S glass films has the effect, as previously mentioned, of decreasing the oscillator strength. Therefore, the addition of silver into the ternary chalcogenide matrix decreases one or other of the quantities on the right-hand side of Eq. (6). Even if Ag photodoping were to change the bonding towards less ionic (considering the electronegativities of the different atoms), this cannot be the major factor, since this factor would increase β. On the other hand, in less ionic materials the smaller s–p splitting increases the parameter N_e [12]. Therefore, in our case of Ge–Sb–S film samples, we assume that the average cation coordination is the factor that is most affected by the addition of Ag to the glassy structure (it should be taken into account that $Z_a = 2$, does not change). Nevertheless, there is an important difference between the Ag-photodoping process of AsS_2 films compared to that in GeS_2 and $GeSe_2$ films. The photodoping of GeS_2 with Ag at concentrations of 16 at.%, destroys $6 \pm 3.5\%$ of the molecular units, whereas in the $GeSe_2$ layers photodoped up to 20 at.% by Ag, $12 \pm 3.5\%$ of the initial number of the $GeSe_{4/2}$ tetrahedrons are destroyed [19]. This disruption of structural units in Ge-based chalcogenide glasses with photodoping and their conservation in As–S glasses, are obviously conditioned by the more rigid structures of the GeX_2 chalcogenide networks. Finally, although the introduction of Sb appears to 'soften' the Ge–S structure (thus, resulting in bond rearrangements and structural changes [18]), it seems reasonable to assume that photodoping with Ag will decrease the effective cation coordination number and, therefore, according to Eq. (6), the dispersion energy will also decrease, as has been found empirically.

6. Conclusions

Photodissolving Ag into the Ge–Sb–S host matrix introduces new Ag–S chemical bonds, with much smaller binding energy than that of the Ge–S and Sb–S bonds, which explains the decrease of the Tauc gap with increasing Ag content. We have analysed the optical-dispersion data using the Wemple–DiDomenico single-effective-oscillator model. The oscillator energy, E_o, varied in proportion to E_g^{opt}, in accordance with the findings of Tanaka [16] and Kosa et al. [17]. On the other hand, we attributed the decrease of the oscillator strength, E_d, with increasing Ag content, to the decrease of the effective cation coordination number, N_c. Lastly, the change in the refractive index between the photodoped and undoped material (around 0.1), for the largest silver concentrations reached in this work, makes the $Ge_{10}Sb_{30}S_{60}$ chalcogenide glass an attractive candidate as optical recording medium.

Acknowledgements

This work has been supported partially by the CICYT (Spain), under the MAT98-0791 project and partially by the Czech Grant Agency, under the 203/99/0420 project.

References

[1] A.V. Kolobov, S.R. Elliott, Adv. Phys. 40 (1991) 625.
[2] T. Wagner, M. Vlcek, K. Nejezchleb, M. Frumar, V. Zima, V. Perina, P.J.S. Ewen, J. Non-Cryst. Solids 198–200 (1996) 744.
[3] Ke. Tanaka, M. Itoh, Optoelectron. Dev. Technol. 9 (1994) 299.
[4] T. Wagner, E. Márquez, J. Fernández-Peña, J.M. González-Leal, P.J.S. Ewen, S.O. Kasap, Philos. Mag. B 79 (1999) 223.
[5] E. Márquez, R. Jiménez-Garay, A. Zakery, P.J.S. Ewen, A.E. Owen, Philos. Mag. B 63 (1991) 1169.
[6] A.V. Stronski, in: G. Harman, P. Mach (Eds.), Proceedings of the NATO Advanced Research Workshop on Microelectronic Interconnections and Assembly, Kluwer Academic, Netherlands, 1998, p. 263.
[7] R. Swanepoel, J. Phys. E 16 (1983) 1214.
[8] R. Swanepoel, J. Phys. E 17 (1984) 896.
[9] E. Márquez, J.B. Ramírez-Malo, P. Villares, R. Jiménez-Garay, R. Swanepoel, Thin Solid Films 254 (1995) 83.
[10] J.C. Manifacier, J. Gasiot, J.P. Fillard, J. Phys. E 9 (1976) 1002.
[11] M. McClain, A. Feldman, D. Kahaner, X. Ying, J. Comput. Phys. 5 (1991) 45.
[12] S.H. Wemple, M. DiDomenico, Phys. Rev. B 3 (1971) 1338.
[13] S.H. Wemple, Phys. Rev. B 7 (1973) 3767.
[14] J. Tauc, in: J. Tauc (Ed.), Amorphous and Liquid Semiconductors, Plenum, New York, 1974, p. 171.
[15] J. Kerr, in: D.R. Lide (Ed.), Chemical Rubber Company Handbook of Chemistry and Physics, 77th Ed., CRC, Florida, 1996.
[16] Ke. Tanaka, Thin Solid Films 66 (1980) 271.
[17] T.I. Kosa, T. Wagner, P.J.S. Ewen, A.E. Owen, Philos. Mag. B 71 (1995) 311.
[18] I.P. Kotsalas, D. Papadimitriou, C. Raptis, M. Vlcek, M. Frumar, J. Non-Cryst. Solids 226 (1998) 85.
[19] A.I. Stetsun, I.Z. Indutnyi, V.G. Kravets, J. Non-Cryst. Solids 202 (1996) 113.